Hunukumbure, M. R., Beach, M. A., Cabrera, M., Vidal, J., & Payaro, M. (2003). 2GHz MIMO channel model from experimental outdoor data analysis in UMTS. In Vehicular Technology Conference 2003 (VTC 2003-Fall), Orlando, FL. (Vol. 2, pp. 1172 - 1176). Institute of Electrical and Electronics Engineers (IEEE). 10.1109/VETECF.2003.1285206

2GHz MIMO Channel Model from Experimental Outdoor Data Analysis in UMTS

Margarita Cabrera, Josep Vidal
TSC Dept. Universitat Politècnica de Catalunya
Barcelona, Spain
{marga,pepe}@gps.tsc.upc.es

Miquel Payaró
Centre Tecnològic de Telecomunicacions de Catalunya
(CTTC), Barcelona, Spain,
miquel.payaro@cttc.es

Mythri Hunukumbure, Mark Beach
Center for Communications Research (CCR)
University of Bristol, U.K,
{mythri.hunukumbure ,m.a.beach}@bristol.ac.uk

***Abstract*— The key objective of this work was to obtain a MIMO model for a Line of Sight (LOS) channel component as well as the covariance matrix for a Non LOS deployment. A Maximum Likelihood Criteria is applied to obtain a LOS Spatial Signature Vector and a NLOS Covariance Matrix derived from channel measurements taken in the 2GHz UMTS spectrum for an urban deployment in Bristol (UK). Different user equipment deployments were considered to represent both LOS and NLOS, as well as static and dynamic (motion) situations. The parameters of interest were estimated from these data and the fitness model was satisfactorily evaluated in all cases. Further, the Kronecker product between transmitter and receiver matrices was evaluated in order to simplify the model, for both, LOS and NLOS cases, including polarization diversity cases..**

***Keywords: MIMO, LOS (Line Of Sight), NLOS (Non LOS), Spatial Diversity, Polarization Diversity*[1].**

I. INTRODUCTION

In order to ascertain the benefits of advanced transmit diversity techniques it is necessary to model the performance of the MIMO channel and thus analyze its influence on the global performance of a system. Previous works, as for instance [1] for 2Ghz and [2] for 5 Ghz, are related with MIMO channel models and based on experimental measurements for different environments.

In this paper, a statistical 2 GHz urban MIMO channel model is proposed based on experimental measurements of the channel response. One of the innovative aspects of the procedure used to obtain the model, consists on applying the ML criteria to real data measures in order to obtain LOS and NLOS terms. The stochastic MIMO channel model here presented is parameterized by second and also first statistical moments and by the LOS Doppler frequency shift between Base Station and Mobile Station equipments. The second statistical moment is the spatial covariance matrix that can be directly related to the diffuse or NLOS components. The first statistical moment represents the LOS component or direct path component, rarely modelled in MIMO propagation channel models. The model considers i) LOS or NLOS presence, ii) Wideband and Narrowband delay spectra and it is supported by measurement data obtained as part of the European IST SATURN (Smart Antenna Technology in Universal bRoadband wireless Networks). Section II describes the MIMO measurement campaign conducted in a small cell urban outdoor environment within the 2GHz UMTS band. In section III the channel matrix to be modeled is presented and the Maximum Likelihood Criteria (MLC) is applied to compute the channel parameters. Section IV shows theoretical discussions about the Kronecker factorization validated by simulations. In section V, the theoretical development is applied about the 2GHz urban measured data obtained and the model fitness is evaluated. Conclusions are given in section VI.

II. MIMO MEASUREMENT CAMPAIGN

The measurement campaign was conducted in Clifton, a dense urban area in Bristol, using the state-of-the-art Medav RUSK BRI vector channel sounder. The measurements occupied a 20MHz bandwidth in the 1910-1930MHz UMTS band. A MIMO configuration of 4 Tx * 8 Rx, consisting of 2 dual polarized UMTS panel antennas at the transmitter and a linear array of 4 dual polarized patch antennas at the receiver, was employed. The antenna separations were 20λ at the transmitter and 0.5λ at the receiver.

The Medav channel sounder is purpose built for SIMO measurements, which can receive and digitally store channel data from 8 antenna ports. In order to carry out MIMO measurements, several hardware customizations were necessary. This included the integration of a high speed multiplexer at the transmitter end to switch through multiple output ports, and digital circuitry that could maintain the synchronism between transmitter and receiver operation.

[1] This work is involved in the EC -IST-199-10322, SATURN project and it is also partially supported by Spanish Government Grants:,TIC2000-1025,and Generalitat of Catalunya Grant 2001SGR 00268

The repetitive AGC burst from the receiver (with a period of 1024μs) was used as the master time reference for transmit antenna multiplexing. With the 4*8 MIMO configuration, two MIMO snapshots can be completed within the time grid as depicted in Figure 1. These two snapshots are well within the outdoor channel coherence times, so these sequential measurements can be assumed to represent true MIMO parallel channels.

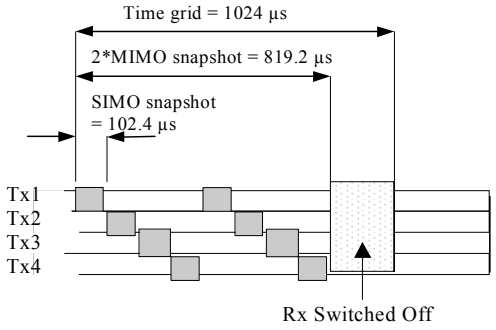

Figure 1. MIMO snapshots- timing diagram

During the campaign, the transmit site was located on a rooftop and the receiving equipment were driven around in a car. Two sets of measurements were taken, one with a stationary car and the other while the car was moving. A single measurement lasted for 4.9 sec, gathering 400 MIMO snapshots. A full description of this campaign can be found in [5].

III. THEORETICAL MODEL AND PARAMETER ESTIMATION

A time delay Complex Impulse Response (CIR) channel is statistically characterized from MIMO measurement files applying a MLC. For a SISO channel the CIR measured at the measure time instant *t* can be represented as a time variant expression:

$$h(t,\tau)=\sum_{l=1}^{L(t)}\alpha_l(t)\exp\left(-j2\pi f_l t\right)\delta\left(t-\tau_l(t)\right) \tag{1}$$

The different paths at he CIR $h\left(t,\tau\right)$ arrive at the receiver at different time delays values τ_l. In (1) *L(t)* represents the number of simultaneous paths impinging in the array, and $\alpha_l(t), f_l, \tau_l(t)$ are respectively the complex amplitude, the Doppler frequency shift and the time delay for the path "*l*", all of them time variant, although the Doppler frequency shift is considered constant along the measure time span. This property is justified given the low mobile speed (inferior to 15 Km/h). The CIR extension in time delay in a UMTS urban environment typically can arrive to some chip periods, (a chip period T_c=0.244 μ sec.).

For a MIMO propagation channel model the number of SISO channels included is $N_c = N_{Tx}.N_{Rx}$, with N_{Tx} denoting the number of sensors at the transmitter end and N_{Rx} the number of sensors at the receiver end. The structure for a MIMO snapshot vector, assumed in this paper is:

$$\mathbf{h}^{\mathrm{T}}\left[t,\tau_s\right]=\left(h(t,\tau_s,1),...,h(t,\tau_s,N_c)\right) \tag{2}$$

For a given time delay value $\tau=\tau_s$ and a given measure time *t* the CIR snapshot is assumed as a complex Gaussian vector. To simplify nomenclature dependence with time delay is not explicitly written along the rest of this section.

$$\begin{aligned}&\mathbf{h}\left[t,\tau_s\right]=\mathbf{h}\left[t\right]=\mathbf{b}e^{j\omega_d t}+\mathbf{z}\left[t\right]\in \mathrm{CM}^{N_c.1};\\&\mathbf{h}\left[t\right]:\mathrm{N}\left(\mathbf{b}e^{j\omega_d t},\mathbf{C}\right)\end{aligned} \tag{3}$$

z[*t*] represents a N_cx1 stochastic, ergodic, temporally white and zero-mean complex (CM: Complex Matrix) Gaussian process with covariance matrix **C**. It corresponds to the diffuse or NLOS component added to the channel noise. $(.)^{\mathbf{H}}$ denotes transpose and conjugate.

$$\mathbf{C}=\mathbf{E}\left[\mathbf{z}\mathbf{z}^{\mathbf{H}}\right] \qquad \mathbf{z}\left[t\right]:\mathrm{N}(0,\mathbf{C}) \tag{4}$$

b is the mean column vector that represents the spatial signature of the arrival signal. Its value is assumed constant along measure time span.

ω_d is a real scalar parameter that represents the LOS Doppler frequency shift in the discrete domain of measure time $t, \omega_d \in \left(-\pi,\pi\right]$. If the frequency Doppler shift in Hz is f_D, $\omega_D = 2\pi f_D T$ where *T* is the measure time sampling time, this is, the time between two consecutive measures of the CIR vector in (3).

For a LOS situation, the signature vector **b** is probably caused by a single direct path. But for NLOS situations if a strong specular component is present in the environment, the spatial signature **b** can be caused by more than one ray. This is an important factor to avoid factorization of vector **b** with angle of arrival or any other parameter. The rest of paths in (1) are NLOS components represented by the time variant diffuse vector $\mathbf{z}\left[t\right]$ in (3).

To compute the different parameters involved in the assumed complex Gaussian model, channel CIR at a time delay τ_s is measured for $t=1:N_t$ obtaining a complex channel CIR matrix **H**. Measure time *t* is supposed to be normalized by the sampling period T, higher than the coherence time.

$$\mathbf{H}=(\mathbf{h}\left[1\right]...\mathbf{h}\left[N_t\right])\in \mathrm{CM}^{N_c x N_t} \tag{5}$$

From (3), the NLOS term in (5) is defined as:

$$\mathbf{Z}=\left[\ \mathbf{z}\left[1\right]\quad \mathbf{z}\left[2\right]\quad ...\quad \mathbf{z}\left[N_t\right]\ \right]$$

and the Doppler shift steering vector as:

$$\mathbf{s}(\omega_d) = \left[1, e^{-j\omega_d}, .., e^{-j\omega_d (N_t-1)}\right]^{\mathbf{T}}$$

The channel matrix modelled in (5) can be expressed as:

$$\mathbf{H} = \mathbf{b}\mathbf{s}(\omega_d)^{\mathbf{H}} + \mathbf{Z} \tag{6}$$

The MLC[4] is applied and the different parameters are sequentially obtained:

- Computation of Doppler frequency directly maximizing Doppler Spectrum, since the expression does only depend on measured data matrix **H**, $\hat{\omega}_d(\mathbf{H}) = \arg\max_{\omega_d}\left(\frac{1}{N_t}\mathbf{s}^{\mathbf{H}}(\omega_d)\mathbf{P}_{\mathbf{H}}\mathbf{s}(\omega_d)\right)$ where $\mathbf{P}_{\mathbf{H}} = \mathbf{H}^{\mathbf{H}}\left(\mathbf{H}\mathbf{H}^{\mathbf{H}}\right)^{-1}\mathbf{H}$ represents the matrix projection on channel matrix column subspace.
- Computation of spatial signature $\hat{\mathbf{b}}(\mathbf{H}, \hat{\omega}_d) = \frac{1}{N_t}\mathbf{H}\mathbf{s}(\hat{\omega}_d)$
- Computation of covariance matrix: $\hat{\mathbf{C}}(\mathbf{H}, \hat{\mathbf{b}}, \hat{\omega}_d) = \frac{1}{N_t}\left(\mathbf{H} - \hat{\mathbf{b}}\mathbf{s}^{\mathbf{H}}(\hat{\omega}_d)\right)\left(\mathbf{H} - \hat{\mathbf{b}}\mathbf{s}^{\mathbf{H}}(\hat{\omega}_d)\right)^{\mathbf{H}}$
- Rice factor is computed in dB from previous averaged estimated statistical moments as $K = 10\log_{10}\left(\frac{|\hat{\mathbf{b}}|^2}{Tr(\hat{\mathbf{C}})}\right)$

IV. LOS AND NLOS COMPONENTS KRONECKER FACTORIZATION

The Kronecker factorization is proposed in this section for the spatial covariance matrix of the NLOS component and as innovative feature for the LOS term (first order statistical moment). For polarization diversity cases a new factorization is proposed consisting in a modified version of the proposed in [3], and it is validated by Monte Carlo simulations and by experimental results.

A. Covariance matrix and mean vector factorization.

The widely assumed transmitter and receiver independence condition leads to a structured form for covariance matrix. For a single polarized MIMO structure [1], [2].

$$\mathbf{C} = \mathbf{C}_{Tx} \otimes \mathbf{C}_{Rx} \tag{7}$$

In (7) the complete MIMO covariance matrix is decomposed as the Kronecker product operator $\otimes$, of the transmitter and receiver covariance matrices: $\mathbf{C}_{Tx} \in \mathrm{CM}^{N_{Tx}xN_{Tx}}$, $\mathbf{C}_{Rx} \in \mathrm{CM}^{N_{Rx}xN_{Rx}}$. We propose in this work two extensions of the property assumed in (7).

i) To generalize this factorization to a dual polarized structure. When each antenna sensor is duplicated at both ends (transmitter and receiver) to a double polarized one, the number of SISO channels is multiplied by four. The polarization effects on the covariance matrix can be decoupled as: $\mathbf{C} = \mathbf{C}_p \otimes \mathbf{C}_{Tx} \otimes \mathbf{C}_{Rx} \in \mathrm{CM}^{4N_c x 4N_c}$. Where $\mathbf{C}_p \in \mathrm{CM}^{4x4}$ is the sub-matrix denoting the polarization effects.

ii) To apply the proposed factorization to the LOS term or spatial signature vector: $\mathbf{b} = \mathbf{b}_p \otimes \mathbf{b}_{Tx} \otimes \mathbf{b}_{Rx} \in \mathrm{CM}^{4N_c}$

B. Simulation Results

The LOS component has been simulated as two symmetric simultaneous rays. The LOS factorization has been evaluated for different angular separation between the two rays and different angles of arrival respect the broadside. Figure 2. shows the error in % produced by the Kronecker factorization applied to the spatial signature vector:

$$\Psi\left(\mathbf{b}, \hat{\mathbf{b}}\right) = \frac{\left\|\mathbf{b} - \hat{\mathbf{b}}\right\|}{\|\mathbf{b}\|}; \quad \hat{\mathbf{b}} = \mathbf{b}_p \otimes \mathbf{b}_{Tx} \otimes \mathbf{b}_{Rx} \tag{8}$$

where $\|.\|$ represents the Euclidean norm.

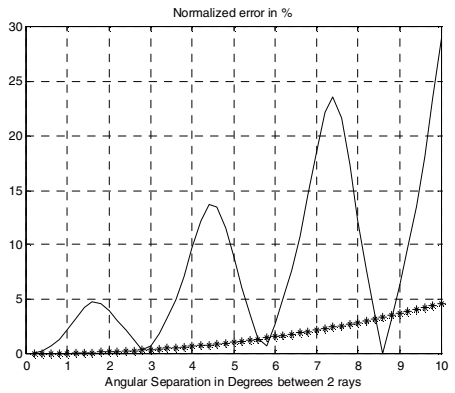

Figure 2. (MonteCarlo Simulations) Mismatch error $\Psi\left(\mathbf{b}, \hat{\mathbf{b}}\right)$ % LOS component has been generated by two scattered rays. $N_{Tx} = 2$ and $N_{Rx} = 2$ dual polarized sensors. Sensor spacing: $d_{Rx} = 0.5\lambda$ (asterisk line) $d_{Tx} = 20\lambda$ (continuous line).

Figure 3. shows the error function $\Psi\left(\mathbf{C}, \hat{\mathbf{C}}\right) = \frac{\left\|\mathbf{C} - \hat{\mathbf{C}}\right\|}{\|\mathbf{C}\|}$ in %, where $\|.\|$ is the Frobenius norm., for three different factorization levels (FL) applied to the covariance matrix:

1. FL1: Kronecker factorization proposed in (2) is only applied to sub-matrices with single polarized sensors at both end (transmitter and receiver) [3]. This situation is represented by "triangles" in the figures.
2. FL2: The covariance matrix is approximated as $\hat{\mathbf{C}} = \mathbf{C}_p \otimes \mathbf{C}_{TxRx}$. In this case only a factorization is applied, in order to identify the polarization factorization effects. It is represented by a "continuous line" in the figures.
3. FL3: The covariance matrix is approximated as: $\hat{\mathbf{C}} = \mathbf{C}_p \otimes \mathbf{C}_{Tx} \otimes \mathbf{C}_{Rx}$. This is the more general case, including approximations 1 and 2. This error results the highest of the three and it is represented in figures by asterisks, but in this case the number of parameters necessary to compute the matrix estimates results the lowest.

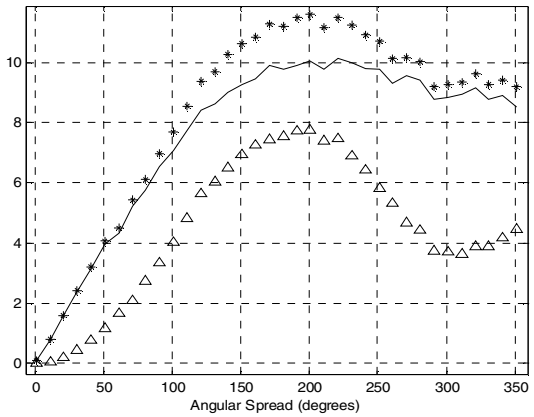

Figure 3. (MonteCarlo Simulations) Mismatch error $\Psi\left(\mathbf{C},\hat{\mathbf{C}}\right)$ %. NLOS component has been generated by 50 scattered rays. Power distribution is considered Laplacian for transmitter end, and Uniform for receiver end. $N_{Tx}=2$ and $N_{Rx}=2$ dual polarized sensors. Sensor spacing: $d_{Rx}=0.5\lambda$ $d_{Tx}=20\lambda$ Cross polarization correlation ρ =-3 dB.

From Figure 2. , Figure 3. and other simulations results it can be concluded that: the Kronecker approximation between transmitter and receiver spatial signatures and covariance matrices will be maintained low (lower than 5% error) for:

- Angular spread maintained lower than 100 degrees.
- Antenna element spacing must be maintained low, about 0.5λ.
- This previous property only has influence on FL1. Logically it doesn't modify the polarization factorization effects.
- The Kronecker approximation improves with the number of scatters. From 25 scatters to up the error in the approximation remains more or less constant.
- In general, the polarization factorization (FL2 and FL3), causes higher errors in the proposed approximation, only moderated for delay spread values under 100 degrees (situation that could be associated to pinhole effect in urban environments). For high spaced sensors the proposed approximation FL3 gives an error similar to the approximation FL1.

V. EXPERIMENTAL RESULTS

A complete set of datafiles were recorded by the partner UoB (University Of Bristol) in the environment of the IST project SATURN . An example is presented (Dynamic LOS), when the maximum likelihood criteria is applied to the real data measured by a $N_{Tx}=2, N_{Rx}=4$ MIMO structure. All sensors share same polarization. A wideband model has been obtained selecting L = 4 paths or samples from the channel matrix.

A. ML Estimates

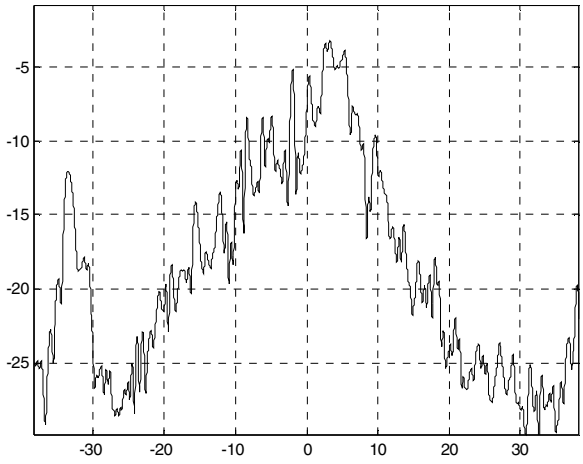

Figure 4. Doppler Spectrum in dB respect to Doppler shift in Hz, for the first path. Dynamic LOS file.

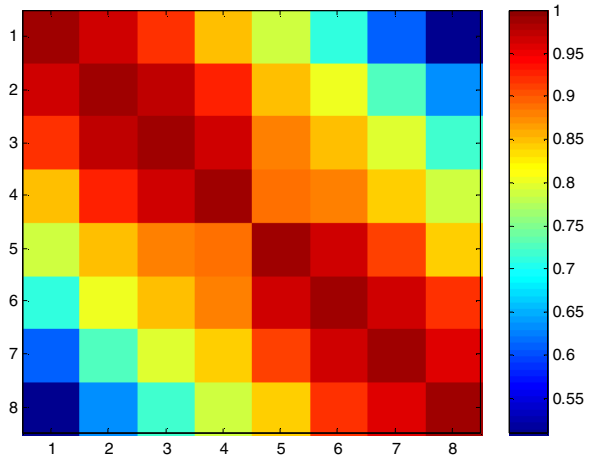

Figure 5. Covariance Matrix $\mathbf{C}(\tau_s) \in \mathrm{CM}^{N_c,N_c}$ absolute value is represented for first path, respec to the matrix index:

$1: Nc = (i_{Tx} - 1)N_{Rx} + i_{Rx}$, $N_c = 8$ A single polarized sub-structure has been extracted from double polarized one. The assumed $\mathbf{C}_{Tx} \otimes \mathbf{C}_{Rx}$ factorization can be inferred from the figure.

B. *Kronecker Factorization error.*

For a LOS Dynamic experimental file, FL errors have been evaluated for the spatial signature vector and the covariance matrix described in sections III and IV. In Table 1, FL1 FL2 and FL3 are applied to estimated data.

TABLE I. FACTORIZATION ERROR

Time Delay	Sp. Signature b FL1 %	Sp. Signature b FL2 %	Sp. Signature b FL3 %	Covariance Matrix C FL1 %	Covariance Matrix C FL2 %	Covariance Matrix C FL3 %
τ_s	3.02	12.96	13.43	5.92	16.18	16.50
$\tau_s + T_c$	4.36	7.78	8.99	6.14	16.63	16.96
$\tau_s + 2T_c$	13.79	33.82	36.38	13.95	21.98	23.45
$\tau_s + 3T_c$	14.82	52.95	53.22	14.13	27.65	28.95

C. *Goodness of fit of the Ricean Model.*

To evaluate the goodness of fit, the recorded real data (assumed to be a Gaussian process in (3)) is previously whitened. In the theoretical model for a MIMO snapshot, the NLOS component can be expressed as:

$$\mathbf{z}[t] = \mathbf{C}^{\frac{1}{2}}\mathbf{w}[t] \tag{9}$$

$\mathbf{C}^{\frac{1}{2}}$ can be obtained by means of a Cholesky decomposition of the matrix $\mathbf{C}$. $\mathbf{w}[t]$ represents a decorrelated random vector such that $E\left[\mathbf{w}[t]\mathbf{w}[t]^{\mathbf{H}}\right] = \mathbf{I}$

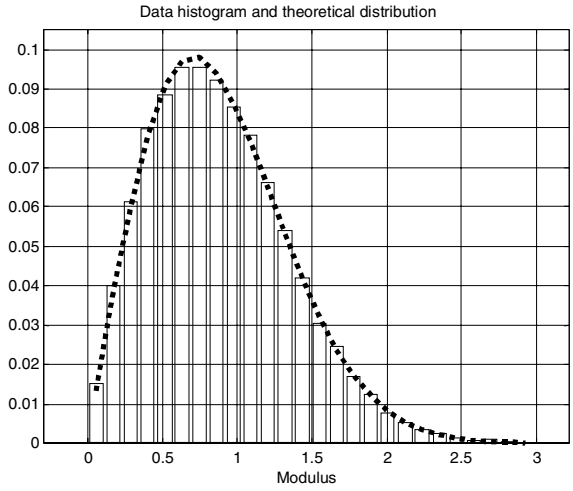

Figure 6. Dynamic Decorrelated process $\hat{\mathbf{w}}[t]$. Absolute value fits into real data samples. Absolute value histogram (bars) and theoretical prediction (dotted line).

If the assumed model fits the real data:

$$\hat{\mathbf{C}}^{-\frac{1}{2}}\left(\mathbf{h}[t] - \hat{\mathbf{b}}e^{j\hat{\omega}_d t}\right) = \hat{\mathbf{w}}[t] \tag{10}$$

$\hat{\mathbf{w}}[t]$ will behave as a white complex zero-mean Gaussian process. Its absolute value distribution fits a Rayleigh distribution (Figure 6.)

VI. CONCLUSIONS

In this work, we have presented a methodology to model the channel for real data MIMO snapshots. A stochastic channel model has also been computed from real data measured in 2GHz UMTS urban environment. The model fitness has been evaluated for all the recorded files during the measures campaign, producing in all the cases satisfactory results.

The model can be generalized to higher order MIMO structures and can be applied to different situations considering LOS or NLOS and static and moving conditions between antennas. In the context of the EC -IST-199-10322, SATURN project, [5] shows a complete analysis of all this kind of situations.

REFERENCES

[1] J. P. Kermoal, L. Schumacher, K. I. Pedersen, P. E. Mogensen, "A Stochastic MIMO Radio Channel with Experimental Validation, " IEEE JSAC Special Issue on Channel and Propagation Models...", vol.20, n6, August 2002, pp. 1211-1226.

[2] K. Yu, M. Bengtsson, B. Ottersten, P. Karlsson, D. McNamara, M. Beach. "Second Order Statistics of NLOS Indoor MIMO Channels Based on 5.2 GHz Measurements" Globecom 2001

[3] J. P. Kermoal, L. Schumacher, F Frederiksen, P. E. Mogensen. "Polarization Diversity in MIMO Channels Experimental Validation of a Stochastic Model and Performance Assessment. Proc. VTC Fall 2001, Atlantic City USA, October 2001.

[4] A. L. Swindlehurst, P. Stoica "Maximum Likelihood Methods in Radar Array Signal Processing. Proc. IEEE, Feb. 1998.

[5] M.Hunukumbure, M. Beach, M. Cabrera, M. Payaró, J. Vidal. EC -IST-199-10322, SATURN Public Deliverable WP321 "MISO/MIMO Radio Channel Models" http://www.ist-saturn.org/